Ribosomal intron-mediated switch governs yeast survival in starvation

Martin Lukačišin[1,2,#], Adriana Espinosa-Cantú[1], Tobias Bollenbach[1,3*]

1. Institute for Biological Physics, University of Cologne, 50931 Cologne, Germany
2. IST Austria, 3400 Klosterneuburg, Austria
3. Center for Data and Simulation Science, University of Cologne, 50931 Cologne, Germany

[#] Present address: Faculty of Medicine, Technion – Israel Institute of Technology, Haifa, Israel

* Corresponding author, t.bollenbach@uni-koeln.de

Abstract

The tight regulation of ribosome content is one of the most important cellular resource-management strategies[1,2]. In the budding yeast, two sets of ribosomal protein (RP) genes, which differ mostly in the presence of introns, contribute to the expression level of ribosomes[3–5]. Despite recent advances on the role of introns under stress and starvation[6–8], understanding the contribution of introns to ribosome regulation remains challenging. Here, combining isogrowth profiling[9] with single-cell protein measurements[10], we found that osmotic stress leads to bimodal expression of the small ribosomal subunit protein Rps22B mediated by intron retention in its transcript. The two resulting yeast subpopulations differ in their ability to cope with starvation. Low Rps22B protein levels implied higher survival rates under long starvation, while high Rps22B levels enabled cells to resume growth sooner after transient starvation stress. Further, yeast growing at high glucose concentrations – similar to those in ripe grapes – exhibit bimodal Rps22B expression when approaching stationary phase. Differential regulation via introns in the RP genes thus provides a way to diversify the population when approaching stationary phase in natural environments. Our findings add regulation of splicing to the known mechanisms employed by yeast to induce phenotypic heterogeneity in changing environments[11,12] and suggest that duplicated RP genes serve to resolve the evolutionary conflict between precise expression control and environmental responsiveness[13].

Main

Free-living cells are frequently challenged by changes in their environment, resulting in a need to allocate their resources accordingly. One of the most important cellular processes to manage is the

production of ribosomes[1,2,14]. Ribosome synthesis, while essential for growth and division, consumes a substantial fraction of cellular resources[15,16]. To assemble into functional complexes, coordinated expression of tens of ribosomal RNA and ribosomal protein (RP) genes is necessary[17]. In the budding yeast, which underwent a whole genome duplication followed by loss or divergence of most duplicated genes[18,19], RPs are largely conserved as duplicates (ohnologs) with high sequence identity[4]. Why evolution may have favoured the retention of RP ohnologs remains an open question; possible reasons include increased gene dosage, genetic robustness towards mutations, and distinct biological roles or differential regulation of the duplicated genes[4,18,20–28]. Recently, it has been suggested that duplicated transcription factors, which are also preferentially retained, might be an evolutionary solution to a trade-off between tight regulation of expression level and responsiveness to environmental changes, such as stress[13]. In this scenario, one ohnolog provides a precise level of protein expression required irrespective of the environment, while the other one generates population heterogeneity, allowing for a flexible response when the environment changes. While the phenotypic effects of deleting the less-expressed copy of duplicated ribosomal genes are usually observed only under stress[22], it is unclear if this paradigm applies to duplicated ribosomal proteins.

The duplicated RP genes in yeast are highly enriched for introns. While fewer than 5% of all yeast genes contain an intron[29], 94 out of 118 (80%) RP genes with an ohnolog do[5]. Differential expression of RP through intronic regulation could expand their functional repertoire, even within the low sequence divergence; hence, introns may be involved in the evolutionary conservation of RP ohnologs[7,23]. Yeast introns in RP genes affect the expression level of the corresponding gene and, in some instances, that of its ohnolog[8,23,30,31]. Concerted intron retention in transcripts occurs in response to stress, suggesting a functional role for splicing regulation in yeast[32]. Such a role is supported by the observation that intron deletion in the budding yeast results in growth alterations under conditions including drug treatment, starvation, or population saturation[6–8]. Introns are thus clearly relevant for adapting to environmental changes; nevertheless, the determinants and functional outcomes of intron-mediated responses remain enigmatic.

Since ribosome synthesis and protein translation are tightly coupled to growth rate[33], it is crucial to dissect cellular responses that are specific to particular stressors from responses to non-specific growth-inhibition when studying the effects of stress on ribosomal function. We have recently established a method for this purpose termed isogrowth profiling[9]. It is based on exposing cells to a combination of two drugs in an antiparallel concentration gradient while keeping the growth rate constant. Analyzing the transcriptome along the growth isobole then enables distinguishing responses specific to each drug, or to their combination, from the general stress and growth inhibition responses.

Here, to explore the role of introns and RPs in stress response, we extend isogrowth profiling from RNA sequencing to single cell protein-level measurements. We found that lithium chloride induces extensive intron retention in RP transcripts, which in turn leads to bimodal expression of Rps22B, a component of the small ribosomal subunit. The two subpopulations exhibit differential fitness under starvation. We show that while yeast in standard rich laboratory growth medium do not exhibit Rps22B-bimodality, cells in medium with high glucose concentration do so as they approach stationarity. Together, these results suggest that yeast has evolved an intron-mediated regulation mechanism of Rps22B to cope with uncertainty regarding possible replenishment of nutrients at the end of exponential growth in a high-glucose environment.

Lithium chloride inhibits splicing of ribosomal protein transcripts

To study the effect of stress on the regulation of ribosomes, we started by investigating the transcriptional response to two growth inhibitors – lithium chloride, a pleiotropic drug inducing cationic and osmotic stress[34], and cycloheximide, an inhibitor of the large ribosomal subunit[33]. Since regulation of ribosomes is sensitive to changes in growth rate and medium composition[33], we used concentrations of the drugs that consistently lowered the relative growth rate close to 50%[9] (**Fig. 1A-B**) and inoculated the drug-free control at a lower cell density so that all samples reach comparable cell density at the time of harvesting (**Fig. 1B**). To determine intron retention, the samples were subsequently ribo-depleted and sequenced without poly-A enrichment (*Methods*). This procedure on the series of drug-mixtures enabled us to observe the specific effects of stressors on intron retention in a way that is not confounded by growth-rate or cell-density effects.

We found that lithium chloride induces extensive intron retention compared to the drug-free control **(Fig. 1C)**. There was no indication that the increase in intron retention was due to changes in growth rate, as no such increase was observed when cells were treated with cycloheximide (**Fig. S1A**). RP transcripts were the functional gene set most strongly affected by this increase in intron retention (BH-corrected hypergeometric test, $p_{adj} = 3 \cdot 10^{-25}$, **Fig. 1C** and **S1B**; *Methods*). Intron retention in RP transcripts did not correlate with their transcript level, suggesting that it is a regulation mechanism independent of that controlling transcription level (**Fig. S1C**). Analyzing RNA-sequencing reads that span the exon-intron junctions confirmed that introns are retained in the transcripts, rather than being spliced out but not degraded (**Fig. S1D**).

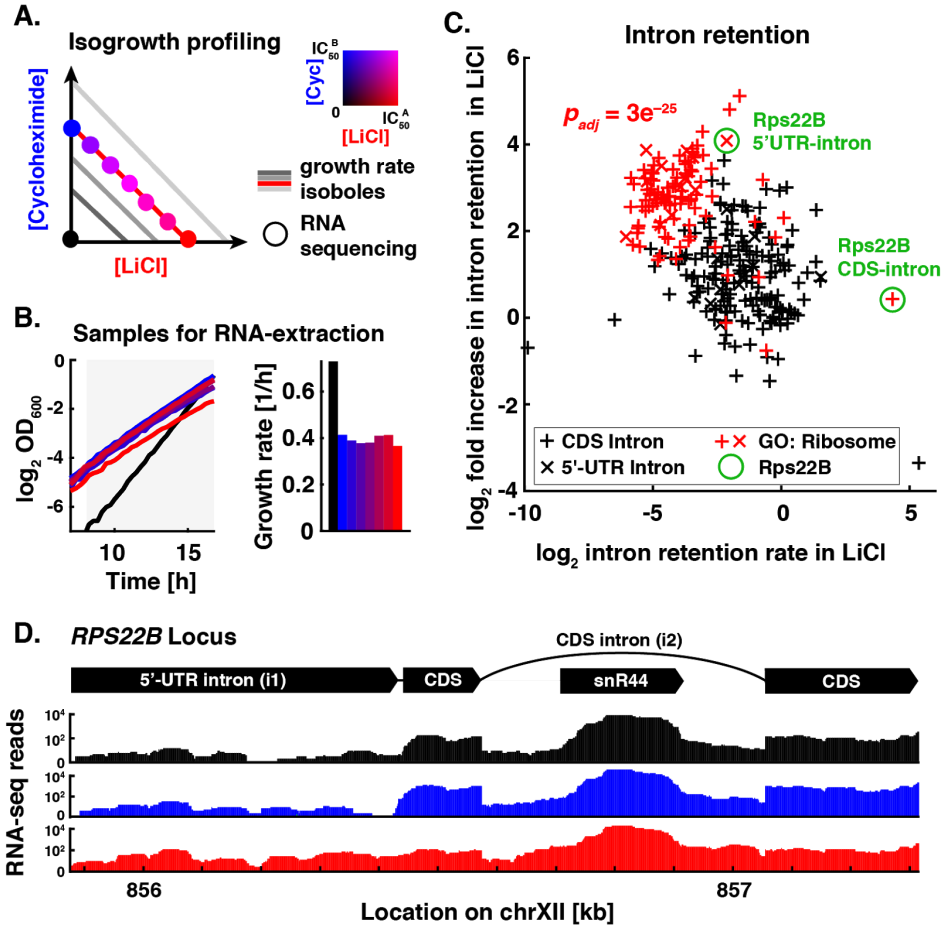

Figure 1: LiCl stress inhibits mRNA splicing of ribosomal proteins.
A. Schematic of isogrowth profiling used to characterize changes of splicing in mRNA. The colored dots indicate the points in the two-drug gradient used to extract total RNA that was subsequently ribo-depleted and sequenced. **B.** Growth curves of samples used for RNA-sequencing. The no-drug control was inoculated at lower density to reach comparable optical density at the time of extraction. Shaded area denotes measurements used to determine the exponential growth rates (right inset). Color code as in A. **C.** Intron retention rate in LiCl (for definition, see *Methods*), relative to no-drug control vs. non-normalized fraction of intron retained. The most significantly enriched GO Cellular Component gene set is displayed in red with the corresponding *p*-value. See also **Fig. S1** for data at other points of the isobole. **D.** RNA sequencing counts for the *RPS22B* locus, color coded as in A. Above: Schematic of the *RPS22B* introns and exons and *snR44* locus according to Saccharomyces Genome Database.

Osmotic stress induces bimodal expression of Rps22B

Rps22B was a clear outlier with respect to intron retention under lithium chloride. Rps22B encodes a component of the small ribosomal subunit and is one of only nine *S. cerevisiae* genes containing two introns[36]. Rps22B contained the 5'-untranslated region (5'-UTR) with the highest increase in intron retention under osmotic stress (**Fig. 1C**) and there appeared to be numerous copies of the coding sequence (CDS) intron of Rps22B, presumably due to a small RNA encoded within the intron that is under separate regulation (**Fig. 1D**, *snR44*). To explore the single-cell behaviour of Rps22B at the protein level, we coupled the rigorously controlled combinatorial drug treatment to flow cytometry using a yeast strain with a GFP tagged Rps22B[10]. Notably, Rps22B exhibited two clearly distinct expression levels at intermediate lithium chloride concentrations (**Fig. 2A**). Other osmotic stressors similarly induced bimodal expression of Rps22B (**Fig. S2A**).

5’UTR-intron retention mediates Rps22B bimodality

While LiCl induced bimodal expression in Rps22B, no such expression pattern was observed for Rps22A, the intronless ohnologue of Rps22B (**Fig. 2A**), whose protein sequence is identical to that of Rps22B except for a single amino acid (**Fig. S2B**). Additionally, auto-regulation of Rps22B protein, dependent on its 5’-UTR intron, was recently reported.[37] Thus, we hypothesized that bimodal expression of Rps22B observed under osmotic stress depends on the presence of one or both introns. Experiments using GFP-translational fusions to Rps22B with seamless deletions of the introns, individually or combined, showed that deleting the 5’-UTR intron abrogates the bimodal expression of Rps22B under LiCl stress (**Fig. 2B**). Both the 5’-UTR-intron deletion and the double-intron deletion strain exhibited higher levels of Rps22B expression under LiCl stress than the original strain. No growth defects that could explain the differences in protein expression between the strains were observed (**Fig. S2C**). This suggests that, upon removal of the 5’UTR-intron, cells under LiCl stress can no longer downregulate Rps22B production via intron retention. The bimodal expression of Rps22B under LiCl stress is mediated by the increased retention of the 5’UTR-intron in its transcript.

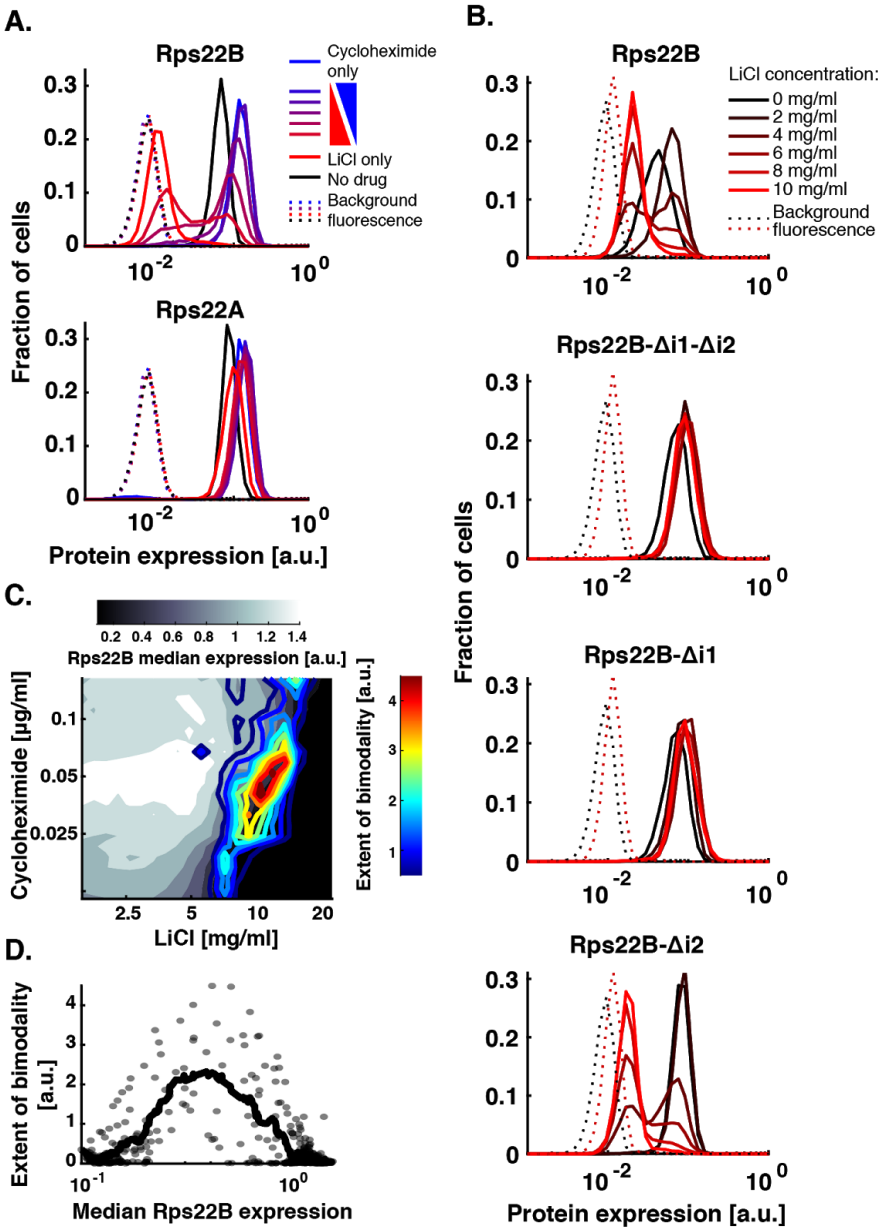

Figure 2: 5'UTR intron mediates bimodal Rps22B protein expression under LiCl, consistent with a bistable regulatory loop.

A. Histograms of flow cytometry measurement of strains with GFP-tagged Rps22B or Rps22A. The ribosomal protein Rps22B, containing the 5'-UTR intron with largest increase in retention due to lithium, exhibits bimodal expression at intermediate lithium concentrations, whereas its ohnologue, Rps22A that contains no introns, does not. See also **Fig. S2** for Rps22B expression in other osmotic stresses. **B.** Histograms of flow cytometry measurements of strains with GFP-tagged Rps22B, with seamless deletion of either or both introns. Notation of introns as in **Fig. 1D**. **C.** The extent of Rps22B bimodality (coloured lines, see *Methods* and **Fig. S4B** for definition), is overlaid on Rps22B median expression (grayscale) in a 2-drug gradient of LiCl and cycloheximide. **D.** The extent of Rps22B protein bimodality as a function of median Rps22B protein expression for all wells in the 2-drug gradient (dots) is shown alongside with running average with a window of 30 data points (line). Rps22B bimodality peaks at a certain level of median Rps22B expression, rather than at a certain growth rate or LiCl concentration. See also **Fig. S4 and S5** for comparison with LiCl-myriocin drug pair.

Single-cell isogrowth profiling uncovers drug-induced protein heterogeneity

To explore the extent to which osmotic or translation stress induce distinct cellular states, as observed for Rps22B, we took advantage of the yeast protein-GFP library[10] containing 4,156 strains with single protein-GFP fusions and performed genome-wide single-cell isogrowth profiling (**Fig. S3A-C**). We profiled the entire library in four conditions (**Table S1**) and selected strains which, on visual inspection, did not show a clear unimodal expression pattern, for further characterization using a more detailed antiparallel gradient (**Table S2**). We found several instances of protein expression heterogeneity resulting from non-specific growth inhibition (**Fig. S3D**) or specifically from either of the stresses (**Fig. S3E**). Cycloheximide induced bimodal expression of Hsp12, the budding yeast persistence marker[38], and of Aro9, an enzyme involved in production of yeast quorum sensing molecule tryptophol[39–41], a trigger for invasive growth in low-nitrogen environment[40]. Lithium chloride induced heterogeneity in Rps9A, another small ribosomal protein subunit containing an intron. Similarly to Rps22B, stress-induced heterogeneity of Rps9A levels was intron-mediated (**Fig. S3F**). Additionally, there was a general trend in which an increase in intron retention in LiCl led to a decrease in the level of the respective protein (**Fig. S3G**). Overall, these observations signify that intron retention is used by the yeast cell to control the protein level and, in the case of Rps9A and Rps22B, also the protein level heterogeneity.

Rps22B expression pattern is consistent with a bistable regulatory loop

A bimodal expression pattern suggests – but does not necessarily imply – an underlying bistable regulatory circuit, such as a positive feedback loop[42,43]. A general hallmark of such a regulatory circuit is the existence of an unstable fixed point. Here, this fixed point would correspond to a protein level at which a small increase or decrease causes the cell to go to one of the two stable fixed points corresponding to high or low expression states[44], respectively. To address if such an unstable fixed point may exist for Rps22B, we explored the Rps22B bimodality in the presence of LiCl stress while using another drug to perturb the growth rate and, as measured, the overall level of Rps22B. We used an automated liquid handling setup that enables continuous monitoring of culture over a fine two-drug gradient distributed over six 96-well microtitre plates[9] (**Fig. S4A**) and at the end of the incubation measured the single-cell protein expression by flow cytometry (*Methods*). We used LiCl in combination with two drugs with disparate mechanisms, the translation inhibitor cycloheximide and a sphingolipid synthesis inhibitor, myriocin[45]. We found that the extent of how clearly the expression levels of the two subpopulations are separated into two peaks depends primarily on the median protein level of Rps22B (**Fig. 2C and S4C-D**), with a maximum at an intermediate level (**Fig. 2D and S4E**). This behaviour is consistent with the existence of an unstable fixed point at this protein level, causing what would be an otherwise log-normally distributed population centered around this point to divide equally into the two presumably stable subpopulations.

Rps22B bimodality leads to differential fitness in starvation

Introns play a key role in preparing the yeast population for starvation[7,32]. Therefore, we hypothesized that the two subpopulations, defined by distinct levels of Rps22B expression, possess differential fitness under starvation stress. To test this idea, we subjected an exponentially growing culture of the Rps22B-GFP strain to LiCl stress using a microfluidic system (*Methods*); following the establishment of bimodality, we replaced the LiCl-containing growth medium with spent medium. In this way, we induced starvation of varying duration, followed by a sudden switch to rich medium (**Fig. 3A**). At first, the spent medium triggered a rapid disappearance of the strong nucleolar signal of Rps22B-GFP (**Movies M1 and M2)**, presumably caused by the redistribution of nucleolar proteins across the cytoplasm upon stress, as occurs in other model systems[46]. Following the switch to rich medium, the nucleolar signal of Rps22B re-emerged in cells that started growing again. Notably, the fitness of cells depended on their Rps22B expression level immediately preceding the starvation stress. Longer starvation stress favoured the survival of Rps22B-lowly expressing cells in that they lysed less frequently than the highly-expressing cells. In contrast, shorter starvation favoured the Rps22B-highly expressing cells in that they tended to resume growth sooner upon nutrient replenishment (**Fig. 3B-F**). This marked diversification of the population observed for Rps22B, with clear fitness effects under a subsequent stress may reflect a bet-hedging strategy[11,12,47].

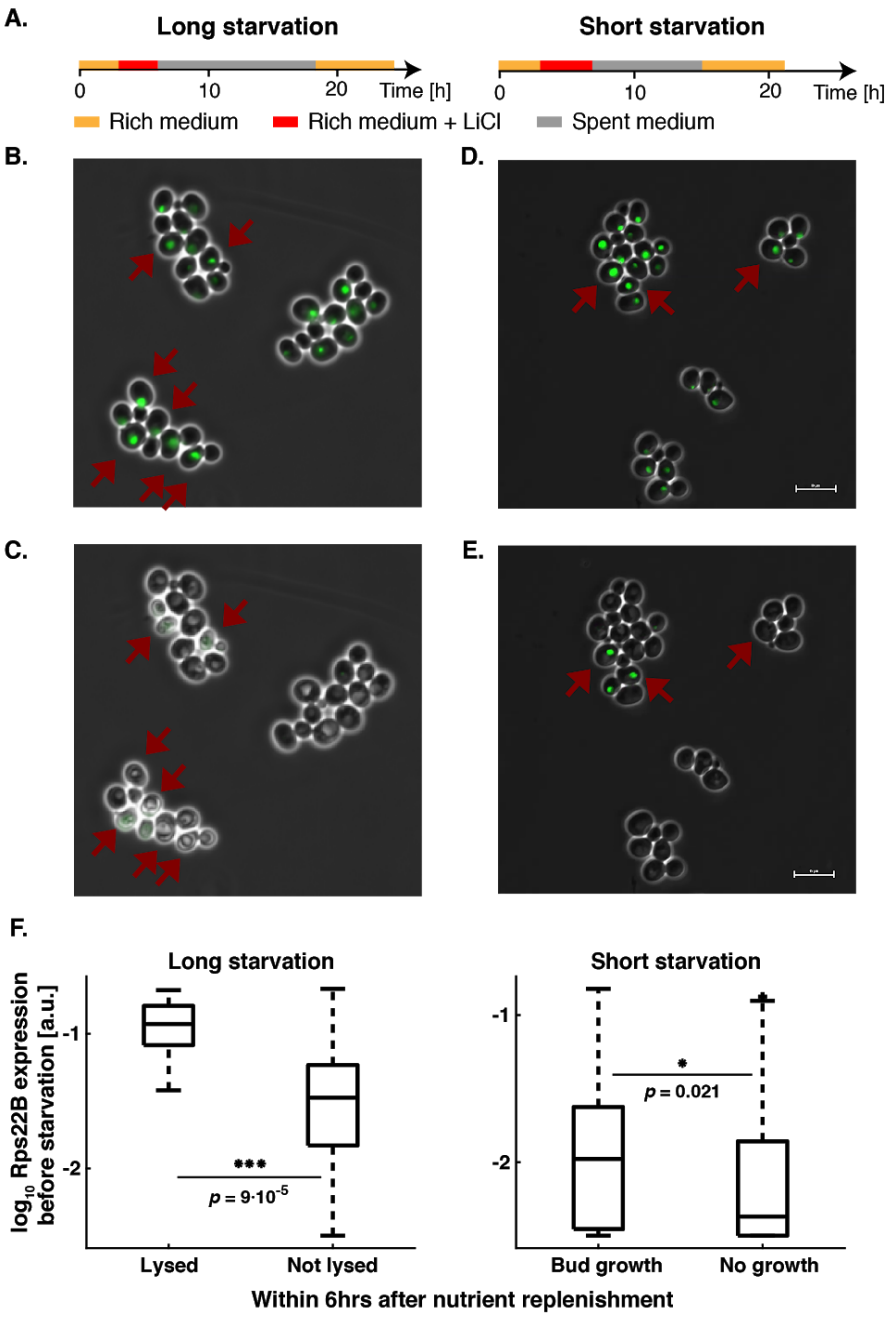

Figure 3: Rps22B expression levels confers selective advantage on cells in starvation stress of varying duration. **A.** Schematic of the media supply used in microfluidic microscopy experiments with the Rps22B-GFP strain. **B-C.** Example micrograph of Rps22B-GFP yeast cells after application of LiCl (B.), showing LiCl induced bimodality of Rps22B expression. The Rps22B high expressing cells marked with dark red arrows lyse following prolonged starvation and nutrient replenishment (C.) **D-E.** Example micrograph of Rps22B-GFP yeast cells after application of LiCl shows lithium induced bimodality of Rps22B expression (D.). Following a short starvation stress and medium replenishment, the Rps22B high expressing cells marked with dark red arrows started budding earlier than other cells (E.). Size bar = 10 µm. See also time-lapse **Movies 1 and 2**. **F.** Quantification of time lapse micrographs from microfluidic starvation experiments. Left panel: Boxplot of Rps22B expression levels in cells that after a long starvation have lysed within 6 hrs after medium replenishment or not, n = 59. Right panel: Boxplot of Rps22B expression levels in cells that after a short starvation have budded within 6 hrs after medium replenishment or not, n = 256. Rps22B expression values between the two panels are not comparable. Mann-Whitney U test was used to determine significance.

(Movie 1)

Movie 1: Long starvation favours Rps22B-low cells in that they lyse less frequently than Rps22B-high cells.
Time lapse microscopy video of Rps22B-GFP yeast strain grown in a microfluidic chamber, flushed with medium as described in **Fig. 3A** left panel. Size bar = 10 μm.

(Movie 2)

Movie 2: Short starvation favours Rps22B-high expressing cells in that they start growing faster after the replenishment of nutrients.
Time lapse microscopy video of Rps22B-GFP yeast strain grown in a microfluidic chamber, flushed with medium as described in **Fig. 3A** right panel. Size bar = 10 μm.

Yeast nearing saturation in high-glucose medium exhibit bimodal Rps22B expression

Bet-hedging strategies are expected to evolve if the eliciting signal is probabilistically followed by stress in which the subpopulations exhibit differential fitness in the natural environment[11,48]. However, yeast nearing saturation, and hence starvation, in standard rich laboratory medium does not exhibit Rps22B bimodality (**Fig. 4A**). Therefore, we wondered if there is a plausible natural setting in which Rps22B bimodality would be triggered just before the onset of starvation. We reasoned that yeast may often be exposed to hyperosmotic sugar concentrations, such as those in ripe fruits. High-glucose elicits osmotic responses that are different from those to salt[49]. Yeast further employs different strategies when entering stationarity depending on the carbon-to-nitrogen ratio[50,51]. Hence, we hypothesized that a high-glucose environment might specifically induce Rps22B bimodality as yeast nears saturation.

To test this idea, we inoculated Rps22B-GFP cultures into a yeast-peptone medium with a high glucose concentration of 20% (w/v), emulating the total hexose concentration in ripe grapes[52], at various initial cell densities. Exponentially growing cells in high glucose medium generally showed less clear bimodal expression of Rps22B-GFP than in LiCl; however, cultures in high glucose medium that were nearing saturation exhibited clearly bimodal Rps22B expression (**Fig. 4B**). This observation suggests that part of the yeast population is attuned to a probabilistic event of nutrient replenishment that can follow growth in a high-glucose environment, while the rest of the population is preparing for starvation.

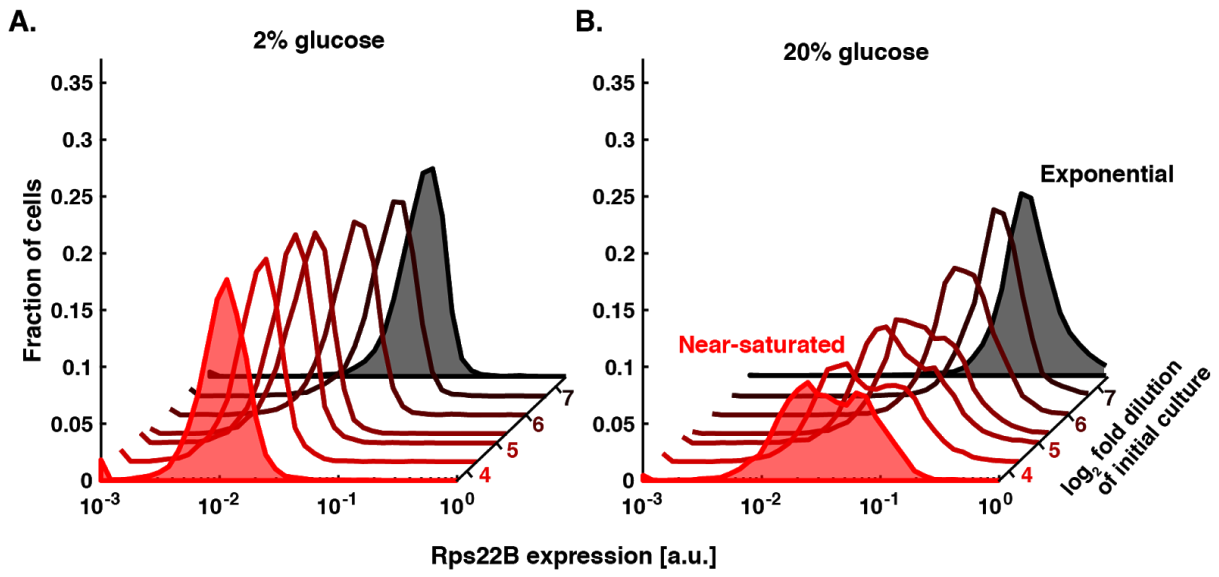

Figure 4: High-glucose environment induces bimodal Rps22B expression as cells nears saturation. Histograms of Rps22-GFP expression as measured by flow cytometry after 10 hrs of incubation in standard rich medium (**A.**), or in yeast extract-peptone medium supplemented with 20% (w/v) glucose (**B.**). Red hue denotes increasing cell density in the initial inoculum. Examples of exponential and near-saturated cultures are highlighted through shading.

Discussion

In the budding yeast, the overall expression level of ribosomal proteins results from two sets of ribosomal protein genes with high amino-acid sequence similarity, often differing in the presence and identity of intronic sequences[8,23]. Here, we uncovered an interplay between the regulation of intron retention and protein expression heterogeneity. We showed that LiCl leads to a widespread retention of introns[53] that is independent of growth rate perturbations and predominantly affects ribosomal protein transcripts. The small ribosomal subunit protein Rps22B showed a bimodal protein expression switch responsive to osmotic stress, mediated by its 5'-UTR intron conserved through *Saccharomycetaceae*[29]. In contrast, its intronless ohnolog Rps22A, exhibited a stable expression level irrespective of stress. This behaviour of the Rps22 gene pair offers a new paradigm to explain the function of introns in duplicated ribosomal protein genes, in that they enable differential and versatile regulation for duplicated genes as an evolutionary trade-off between environmental responsiveness and precise regulation[13].

We found that population diversification due to bimodal expression of Rps22B leads to differential fitness of these subpopulations in the face of starvation stress of varying duration. Reminiscent of bet-hedging strategies[11], we found that in high glucose medium, yeast populations diversify in Rps22B expression as they enter stationary phase, as if anticipating a probabilistic replenishment of nutrients. Why should such a behaviour have evolved for a high-glucose environment, but not manifest at glucose levels present in the standard laboratory "rich" medium? One plausible scenario is that high glucose concentration, for yeast living on the skin of grapes, is an environmental signal that the fruits are ripening and bursting. Osmotic bursting of fruits is known to follow a probabilistic trajectory over time[54] and is known to happen predominantly during rainfall[55]; hence, in a cluster of grapes, vigorous yeast growth due to bursting of one of the berries might be followed by nutrient replenishment due to bursting of a neighbouring berry, determined by the probabilistic aspects of rain duration and intensity.

The fact that we found osmotic stress-induced, intron-mediated phenotypic heterogeneity only for Rps22B and Rps9A, while most other pairs of duplicated ribosomal proteins also contain at least one intron, is intriguing, especially since the effect of introns on protein expression level has been reported for other ribosomal proteins in the budding yeast[8,56]. It is thus tempting to speculate that for other ribosomal proteins, there might exist other levels of osmotic stress, or other stressors altogether, that would trigger population diversification with respect to the expression level of a given ribosomal protein. Such a set of diversification mechanisms could then present a versatile stress toolkit for the yeast population bracing against continued stress, at the same time maintaining a small, stress-sensitive subpopulation poised to rapidly exploit a short window of fitness advantage should the stress suddenly disappear. Our study thus highlights the need of studying the intronic regulation of population diversification and demonstrates the utility of using graded, growth-rate controlled perturbations.

Methods

Transcriptional isogrowth profiling

For isogrowth RNA sequencing, *S. cerevisiae* strain BY4741 was grown in 7 conditions of varying ratios of LiCl (Sigma Aldrich, L9650) and cycloheximide (Sigma Aldrich, 37094), ensuring 50% growth inhibition, and in YPD [yeast extract (Sigma Aldrich cat. No. Y1625) 1% w/v, peptone (Sigma Aldrich cat. No. 91249) 2% w/v, dextrose (Sigma Aldrich cat. No. D9434) 2% w/v] containing no drug (Table 1). The frozen stock was diluted 130-times into drug containing wells and 100-times more into wells without drug. The cells were incubated for ~17 hrs to an absorbance of ~0.1 on the 96-well plate, corresponding to OD_{600}~0.5. Cells were then harvested and the RNA extraction was performed using RiboPure RNA Purification Kit for yeast (Thermo Scientific, AM1926). The extracted RNA was sent to the Next Generation Sequencing Facility of the Vienna Biocenter Core Facilities, where it was rRNA depleted using Illumina Ribozero Yeast Kit, multiplexed using Illumina True Seq adapters, single-end 50bp sequenced using Illumina HiSeqV4 and demultiplexed.

Condition (as labeled in Fig. S1)	Cycloheximide [µg/ml]	LiCl [mg/ml]
1	0.11	0
2	0.095	1.2
3	0.083	2.5
4	0.069	4.1
5	0.049	5.9
6	0.026	7.7
7	0	8.5

Table 1: Concentrations of drugs used for the RNA-isogrowth profiling

Intron retention analysis

The reads resulting from sequencing were aligned to the annotated reference *S. cerevisiae* genome R64-2 using TopHat[57]. The reads mapping to introns or CDS of intron-containing genes were quantified using featureCounts[58] using custom produced .saf files extracted from the reference .gff annotation file. The intron retention rate was calculated as the ratio of intron counts normalized to the intron length over the CDS counts normalized to the length of the CDS region. For genes containing multiple introns, the introns were treated jointly for CDS introns and separately for 5'-UTR introns.

For the analysis shown in Fig. S1D, first the number of contiguous reads (no mismatches allowed) overlapping the individual intron ends was determined. This count was then averaged between 5' and

3'-end of the intron ends and divided by the read length (50bp). The intron retention rate was then calculated as the ratio of the resulting value over the CDS counts normalized to the length of the CDS region.

For GO enrichment analysis, intron-containing genes were ordered into a ranked list based on the fold-change increase in intron retention in LiCl compared to the no-drug control, either in decreasing (Fig. 1C) or increasing order (Fig. S1B). The ranked list was then analysed using GOrilla[59], for either Cellular Component or Biological Process, respectively. The adjusted *p*-values reported here correspond to the false discovery rate reported by GOrilla.

Screening the entire yeast protein-GFP library for drug-induced bimodality

The whole yeast protein-GFP library[10], contained in 43 96-well microplates, was screened for drug-induced bimodality by culturing in four conditions: YPD medium containing no drug, cycloheximide, LiCl, or a combination of LiCl and cycloheximide. The screen was divided into 6 experimental batches. In every batch, up to 9 plates of the library were processed, with the same strain being cultured in four conditions on the same day and on the same microtitre plate, giving rise to up to 36 microtitre plates per experiment. Before the experiment, empty microtitre plates and YPD medium were pre-incubated at 30°C to ensure reproducibility of gene expression measurements. LiCl, cycloheximide, or a mixture of the two, were diluted with YPD to a final concentration needed to achieve 40% inhibition and ensuring that in the mixed condition, the LiCl and cycloheximide were mixed in an equipotent manner, meaning that on their own they both elicited approximately the same (smaller) growth inhibition (Table 2). The drug solutions were pipetted row-wise into a 96-well microtitre plate, including a drug-free YPD control, enabling the cultivation of 24 strains in 4 conditions per microtitre plate. The library plates stored at -80°C were thawed and, using an electronic multi-step multi-channel pipette, 1.5 µl saturated glycerol stock of the corresponding strain was inoculated into each drug-containing well and 0.2 µl of the saturated glycerol stock was inoculated into drug-free YPD as a control. The smaller inoculum size for the drug-free control was designed to ensure that the final cell density at the end of the experiment is comparable to that of the drug-containing wells. Plates were incubated for ~14 hrs in an automated incubator (Liconic StoreX) kept at 30°C, >95% humidity, vigorously shaken at >1000 rpm. During the incubation, OD600 was measured every ~45 min in a Tecan Infinite F500 plate reader. In addition to shaking during incubation, directly before each measurement, plates were shaken on a magnetic shaker (Teleshake; Thermo Scientific) at 1100 rpm for 20 s. The growth rates were inferred by fitting a line to the log-linear part of OD_{600} measurements between 0.01 and 1.

After incubation, the yeast cells in 96-well microtitre plates were twice: centrifuged at 1050 g for 3.5 min and resuspended in ice-cold Tris-EDTA buffer by vigorous shaking at 1000 rpm on a Titramax shaker for 30 s. After another centrifugation at 1050 g for 3.5 min, the cells were resuspended in 80 µl of Tris-EDTA and immediately stored at -80°C. On the day of the flow cytometry measurement, the plates were thawed on ice for ~3 hrs and kept on ice until the measurement. The fluorescence was measured for 10,000 cells using BD FACS Canto II equipped with a high-throughput sampler. The green fluorescence measured in FITC-H channel was normalized to the forward scatter FSC-H channel.

Strains exhibiting bimodality, minor peaks, or prominent changes in gene expression at visual inspection of the expression histograms were manually selected for a more detailed screen. The

selected strains were re-streaked from the yeast protein-GFP library microtitre plates onto YPD-agar plates and single clones for each strain were picked and cultured in a 96-well microtitre plate to saturation. Glycerol was added to a final concentration of 15% and the plates were frozen. The plates were screened in 8 conditions and analysed using flow cytometry in a way analogous to that described above. The identity of the relevant strains − Rps22A, Rps22B, Aro9, Hsp12, Cit1 and Tdh1 − was confirmed by PCR and gel electrophoresis as reported before[10], using a common F2CHK reverse primer and strain specific oligos taken from (https://yeastgfp.yeastgenome.org/yeastGFPOligoSequence.txt). The strain Smi1 appeared bimodal in the screen; however, its identity could not be confirmed as above. The identity of other strains was not tested.

Condition	Cycloheximide [µg/ml]	LiCl [mg/ml]
Cycloheximide only	0.10	0
Cycloheximide + LiCl	0.050	6.3
LiCl only	0	13.5
YPD only	0	0

Table 2. Concentrations of drugs used in the whole yeast protein-GFP library isogrowth screen.

Construction of GFP-labeled intron deletion strains and flow cytometry experiments

The seamless intron deletion strains for Rps22B (Rps22B-Δi1-Δi2, rps22bDi_JPY138F4; Rps22B-Δi1, rps22bD1i_MDY125A4; Rps22B-Δi2, rps22bD2i_MDY125A9) and Rps9A (Rps9A-Δi, rps9aDi_MDY133H8), as well as the parental haploid strain WT_JPY10H3 (Mat**a** ura3Δ0 lys2Δ0 leu2Δ0 his3Δ200) were a kind gift of Julie Parenteau and Sherif Abou Elela[7]. Intron deletion strains were labeled with GFP fused to the protein of interest following homologous recombination of the PCR-amplified fluorescent marker from the matching yeast protein-GFP library strains. To achieve this, the DNA of the Rps22B-GFP and Rps9A-GFP strains from the library was extracted using Yeast DNA Extraction Kit (Thermo Scientific, 78870). PCR Amplification of the GFP label with 40 base pairs flanking sequences was done using the corresponding F2 and R1 pair of primers from Huh et al (https://yeastgfp.yeastgenome.org/yeastGFPOligoSequence.txt) in the following reaction conditions: 2 ng/ml of DNA in a final mix of 20 µl, with 0.4 units of Phusion High-Fidelity DNA polymerase (Thermo Fisher Scientific, Cat# F530SPM), 4 µl of 5x Phusion HF buffer, 0.2 µM dNTPs, and 0.5 µM primers. PCRs were incubated for 3 min at 98°C, followed by 34 cycles of 98°C for 30 sec and 72°C for 2.5 min, and a final incubation at 72°C for 5 min. The resulting PCR products were transformed into the parental WT_JPY10H3 and Δi strains as in Howson et al.[60], selecting on SD -HIS agar plates (Takara Bio, 630411; Diagonal GmbH&CoKG, Y1751). The correct genomic context insertion of GFP of single colonies was confirmed by PCR using a combination of primers which also allowed the confirmation of the intron deletion strain. To confirm the Rps22B-GFP fusions in Rps22B-Δi and the WT_JPY10H3

strains, we used primers rps22b-899F 5'-CCGTTATTCTTCTCGCAACC-3' binding upstream the 5'-UTR intron and RPS22B-CHK[60] 5'- ACTAGATGGTGTGATCGGGC-3' binding in the CDS-intron sequence in combination with the reverse primer F2CHK[60] 5'- AACCCGGGGATCCGTCGACC-3', complementary to the GFP sequence. To confirm the Rps9A-GFP fusions in the Rps9A-Δi and WT_JPY10H3 strains, we used rps9a-800F 5'- GTTCGATTTCTTGGTCGGACGC-3' upstream the open reading frame and F2CHK. Once the successful construction of the GFP reporter strains was confirmed, 20 µl of saturated overnight cultures were inoculated into 96-well microtiter plates containing 180 µl of YPD with the respective concentration of LiCl. The microtiter plates were incubated at 30°C and continuous shaking at 900 rpm on a Titramax shaker for 7 hrs, and harvested and measured on a flow cytometer as described above.

Measurement of Rps22B expression in detailed 2D drug gradients

The re-inoculation setup, as reported previously[9], in conjunction with flow cytometry measurements was used to measure Rps22B expression in detailed 2D gradients of LiCl and cycloheximide, and LiCl and myriocin (Sigma Aldrich, M1177). In brief, *Saccharomyces cerevisiae* strain with RPS22B gene fused to GFP protein from ORF-GFP library[10], was grown in YPD broth in a conical flask overnight and then distributed into a 96-well plate. A customized robotic setup (Tecan Freedom Evo 150) with 8 liquid handling channels and a robotic manipulator was used to produce a two-dimensional discretised two drug 24x24-well gradient in YPD spread over six 96-well plates and to inoculate the yeast overnight culture to final liquid volume in the well 200 µl and final absorbance 0.03 on the 96-well plate, corresponding to standardised optical density at 600 nm of 0.15. Working drug solutions were prepared either by adding respective amounts of concentrated DMSO drug stocks thawed from -20°C storage (no refreezing) previously prepared from stock chemicals (cycloheximide and myriocin), or by dissolving directly in YPD and sterile-filtering (LiCl). The six plates were incubated for three iterations, each lasting ~8 hrs. After the incubation the cells were harvested and measured using flow cytometry as described above. Rps22B protein bimodality was quantified as the depth of the trough on the Rps22B protein single-cell expression histogram, that is the y-axis distance between the trough and the lower of the two peaks. To this end, Matlab function *findpeaks* was used to determine the prominence of the peak that was created from the trough through inversion of the histogram values.

Time-lapse imaging of Rps22B-GFP strain during starvation

The ORF-GFP library Rps22B-GFP strain was inoculated into YPD, 30°C shaking overnight. In the morning, the culture was diluted 20-fold into 6 mg/ml LiCl in YPD and incubated for another ~5 hrs. The resulting culture was diluted 10-fold and loaded to the CellASIC ONIX2 haploid yeast microfluidic plates (MerckMillipore) at 55 kPa pressure and the corresponding media were flushed in a timed sequence at 10 kPa pressure. Spent medium was produced by incubation of the Rps22B-GFP strain in YPD medium for 7 days with subsequent sterile filtration. The specimen was imaged every 5 min at multiple locations with Nikon Eclipse Ti inverted microscope using a 100x oil objective in a 30°C cage incubator. The micrographs of yeast from just before the starvation stress were segmented and fluorescence-quantified using CellProfiler[61] and the fluorescence readout was $\log_{10}$-transformed assuming $10^{-2.5}$ as a background fluorescence value. The time-lapse images were then visually scored to determine which cells budded/lysed after the replenishment of nutrients.

Rps22 bimodality in other osmotic stresses and in high glucose

The ORF-GFP library Rps22B-GFP cultures were inoculated into YPD medium, YPD containing 0.6M NaCl, 2M KCl (Sigma Aldrich, S3014 and P9541 respectively) or to a yeast-peptone medium with 5, 10 or 20% (w/v) glucose (Sigma Aldrich, G8270). In order to measure fluorescence intensity of cells from different cell density and growth stages, 6 technical replicas were prepared in independent microtiter plates, each with the same conditions and cultures started with a gradient of initial inoculum sizes; in this way, each plate accounted for the stress array with different cell density and could be incubated and analyzed at different time-points. To achieve this, saturated overnight cultures were diluted with YPD in a 4/5 serial dilution (i.e. 4ml were transferred to the final volume of 5ml) to obtain $(4/5)^0$ to $(4/5)^{23}$ dilutions. Subsequently, 15 µl of cell dilutions were inoculated in 185 µl of media. Plates were incubated at the Liconic StoreX and kept at 30°C, >95% humidity, shaken at ~500 rpm. Plates were processed at 8, 12, 16, 20 and 24 hours after inoculation with an automated robotic system consisting of a ACell System (HighRes Biosolutions) integrated with a Lynx liquid handling system (Dynamic Devices), a plate reader (Synergy H1, BioTek), and a CytoFLEX flow cytometer (Beckman Coulter). First, plates were shaken and measured as described above to obtain the OD_{600} values. Cultures were then transferred to a new plate and diluted when necessary to an absorbance of ~0.3 with Tris-EDTA buffer in order to avoid high cellular densities and measured by flow cytometry. After taking samples, the plate was discarded.

Data availability

The RNA sequencing data are available in Gene Expression Omnibus under accession no. GSE155060. The processed flow cytometry data are available as Supplementary Table 1 and 2 accompanying this manuscript.

Acknowledgements

We would like to thank the IST Austria Life Science Facility for the support of the liquid handling robot. The Bioimaging Facility at IST Austria, and Jeffrey Power and Berenike Meier at the University of Cologne for the support of flow cytometry experiments. Lucas Horst for the development of the automated cytometry experiments in Cologne. Julie Parenteau and Sherif Abou Elela for providing us with Rps9A and Rps22B seamless intron deletion yeast strains. The members of Bollenbach group for technical support. Mike Springer, Daria Siekhaus, Gašper Tkačik and all the members of the Bollenbach group for fruitful discussions. Karin Mitosch and Marta Lukačišinová for the critical reading of our manuscript. This work was supported in part by Austrian Science Fund (FWF) standalone grant P 27201-B22 (to T.B.), HFSP program Grant RGP0042/2013 (to T.B.), EU Marie Curie Career Integration Grant No. 303507, and German Research Foundation (DFG) Collaborative Research Centre (SFB) 1310 (to T.B.). A.E.C is supported by a Georg Forster fellowship from the Alexander von Humboldt Foundation.

Author contributions

Conceptualisation: M.L. and T.B.; Investigation: M.L. and A.E.C.; Writing original draft: M.L.; Writing - review and editing: M.L., A.E.C., T.B.; Supervision: T.B.; Funding acquisition: T.B.

Supplementary figures

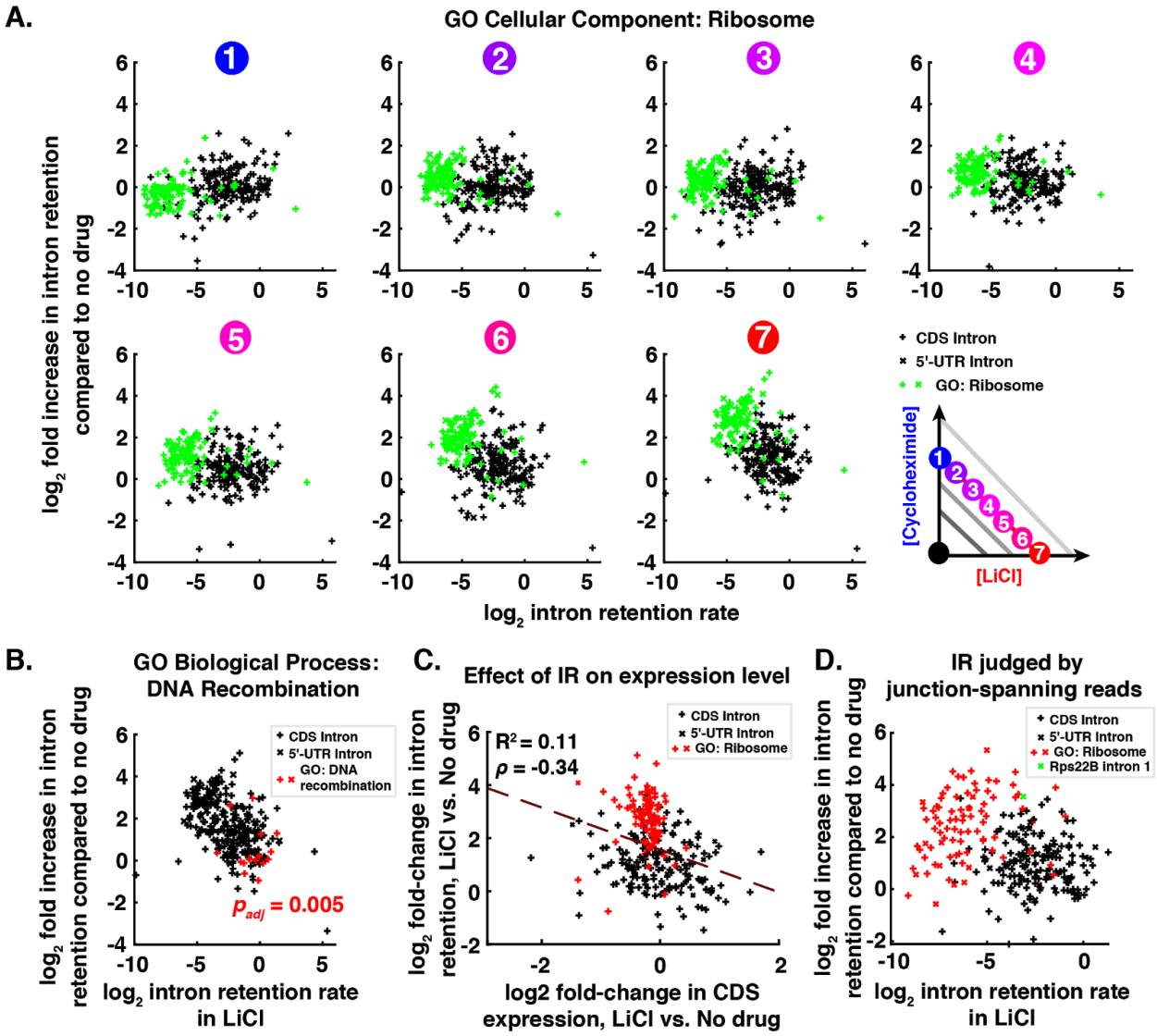

Figure S1: Introns in ribosomal proteins facilitate ribosomal protein response to LiCl stress. Refers to Figure 1. **A.** Intron retention rates along the 50% growth isobole of cycloheximide-LiCl drug combination. Introns contained in the genes belonging to the most significantly enriched GO Cellular Component with no offspring term as determined for the upper end of relative intron retention increase in LiCl are highlighted in green. For quantification of intron retention rates from RNA sequencing data and gene enrichment analysis refer to *Methods*. **B.** Intron retention rate in LiCl (as in panel 7 in A). The introns from genes belonging to the GO Biological Process term most significantly enriched in the lower end of the relative increase in intron retention is displayed in red, with the corresponding adjusted *p*-value shown. **C.** Change in intron retention (IR) in LiCl compared to no drug for individual introns does not correlate with the expression level of the corresponding RNA as gauged by the RNA-seq read counts in coding region (CDS). Linear model was fitted over all introns; low values of Pearson correlation ρ and R^2 are indicative of intron retention being independent from regulation of transcript level. **D.** Analysis of intron retention using only the sequencing reads overlapping the exon-intron junction as the proxy for intron retention rate (see *Methods*). The good agreement with the analysis being performed using all reads in the intron (panel A) shows that introns are being retained within the transcripts rather than just being spliced and non-degraded.

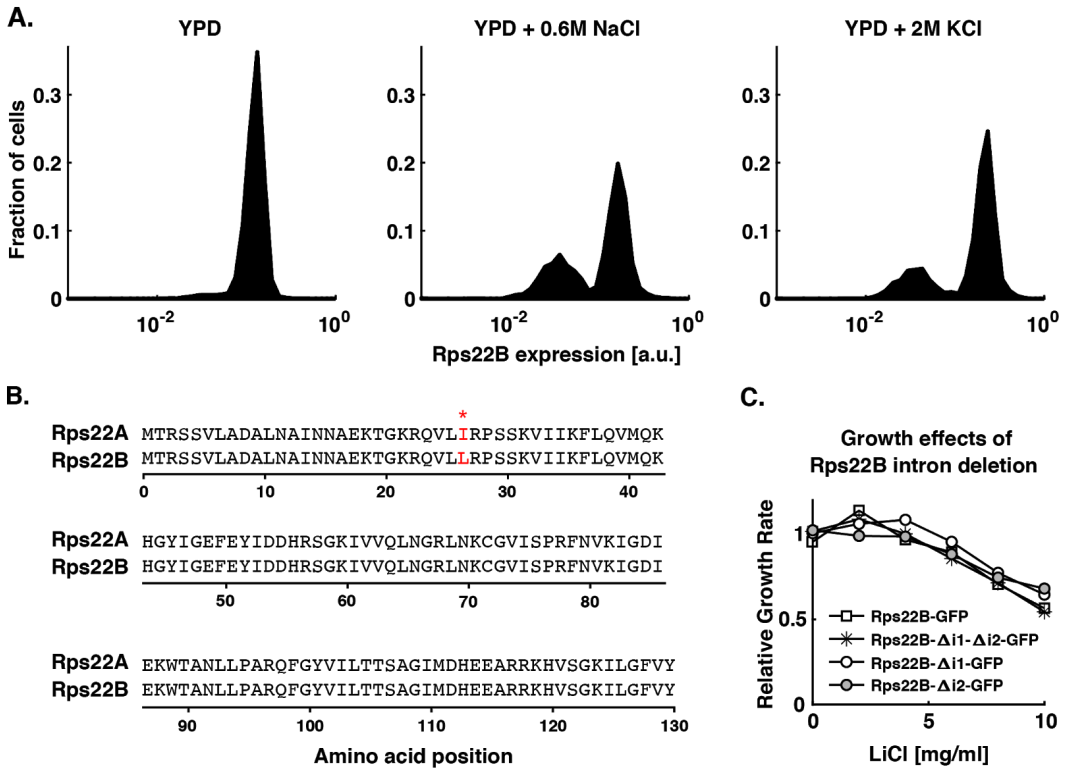

Figure S2: Osmotic stress induces bimodal expression in Rps22B. Refers to Figure 2.
A. Histograms of Rps22B-GFP expression in NaCl and KCl as measured by flow cytometry during exponential growth phase after 16 hrs of incubation in respective conditions. **B.** Protein blast for Rps22A and Rps22B. Red asterisk denotes the single difference between the amino acid sequences. RefSeq entries NP_013471.1 and NP_012345.1 are shown for Rps22A and Rps22B proteins, respectively. **C.** Changes in growth rate due to intron deletion in Rps22B-GFP reporter strain cannot account for differences in Rps22B expression pattern. Growth rates for respective strains are shown relative to the mean of their growth rates in no drug control.

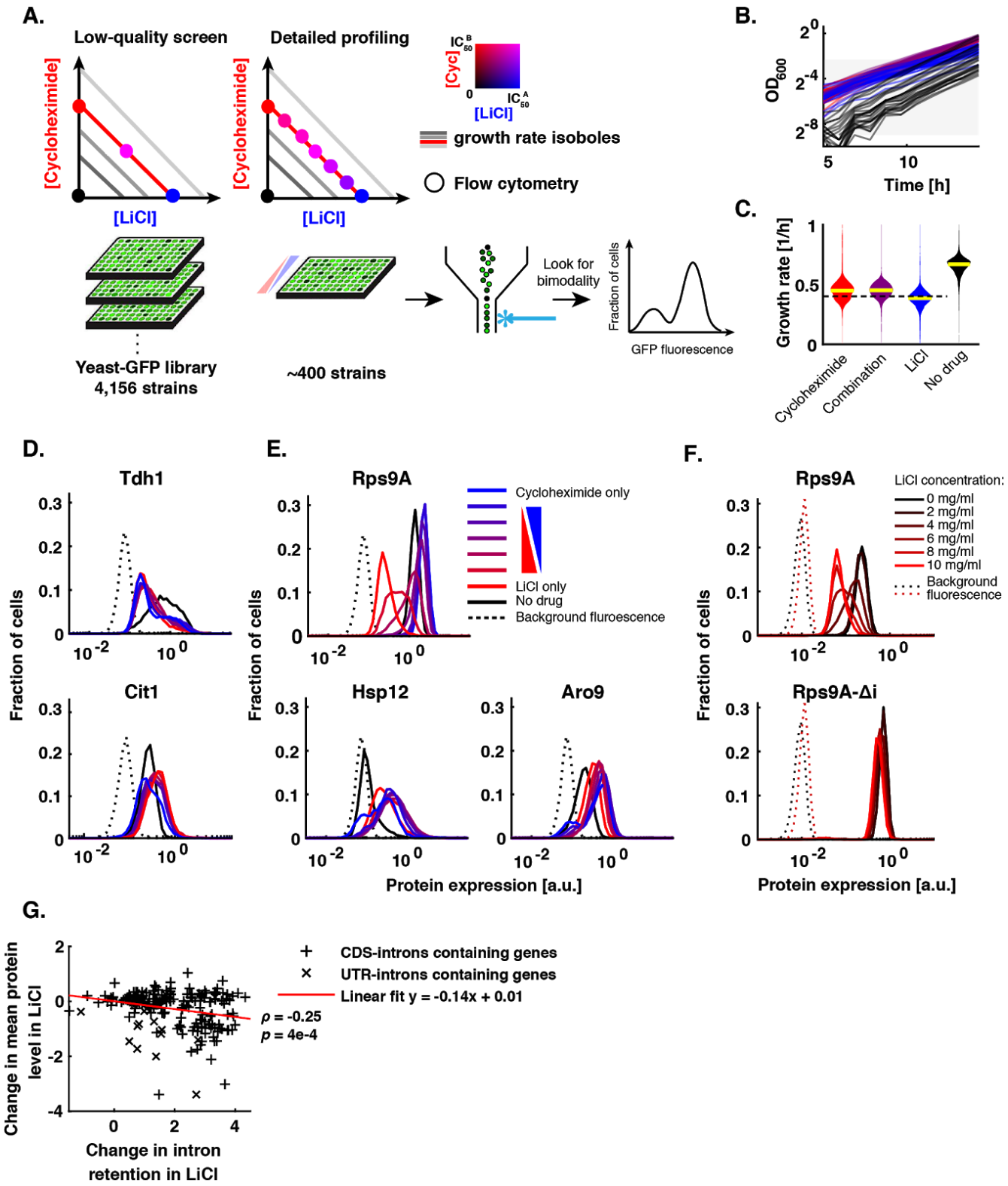

Figure S3: Single-cell isogrowth profiling uncovers drug-induced cellular states. Refers to Figure 2.
A. Schematic showing the experimental strategy for single-cell isogrowth profiling. Using flow cytometry, the entire yeast protein-GFP library was screened in four conditions: no drug, each of the two drugs alone at 40% inhibition, and an equipotent combination of drugs at the same total inhibition. About 10% of genes which showed an unusual expression pattern were restreaked and subjected to a more detailed screen in 8 conditions. **B**. Example growth curves of one 96-well plate with 24 strains each in 4 conditions. Note that the inoculum of the no-drug condition was decreased in order to achieve comparable final cell density at the time of harvesting. The shaded area denotes the OD range used for fitting of growth rates.

C. Violin plot showing the distribution of growth rates for the initial screen over the entire library. The dashed line indicates 40% growth inhibition. **D.-E.** Single-cell GFP intensity histograms of protein-GFP fusion strains. Proteins with bimodal expression induced by growth inhibition by both LiCl and cycloheximide (D.) or specifically by either drug (E.) are shown. **F.** Intron deletion in Rps9A abolishes the LiCl-induced bimodality. **G.** Change in intron retention in LiCl compared to equal inhibition by cycloheximide as judged by RNA-sequencing is inversely related to the change in mean protein level in LiCl as determined by flow cytometry. ρ – Pearson correlation coefficient.

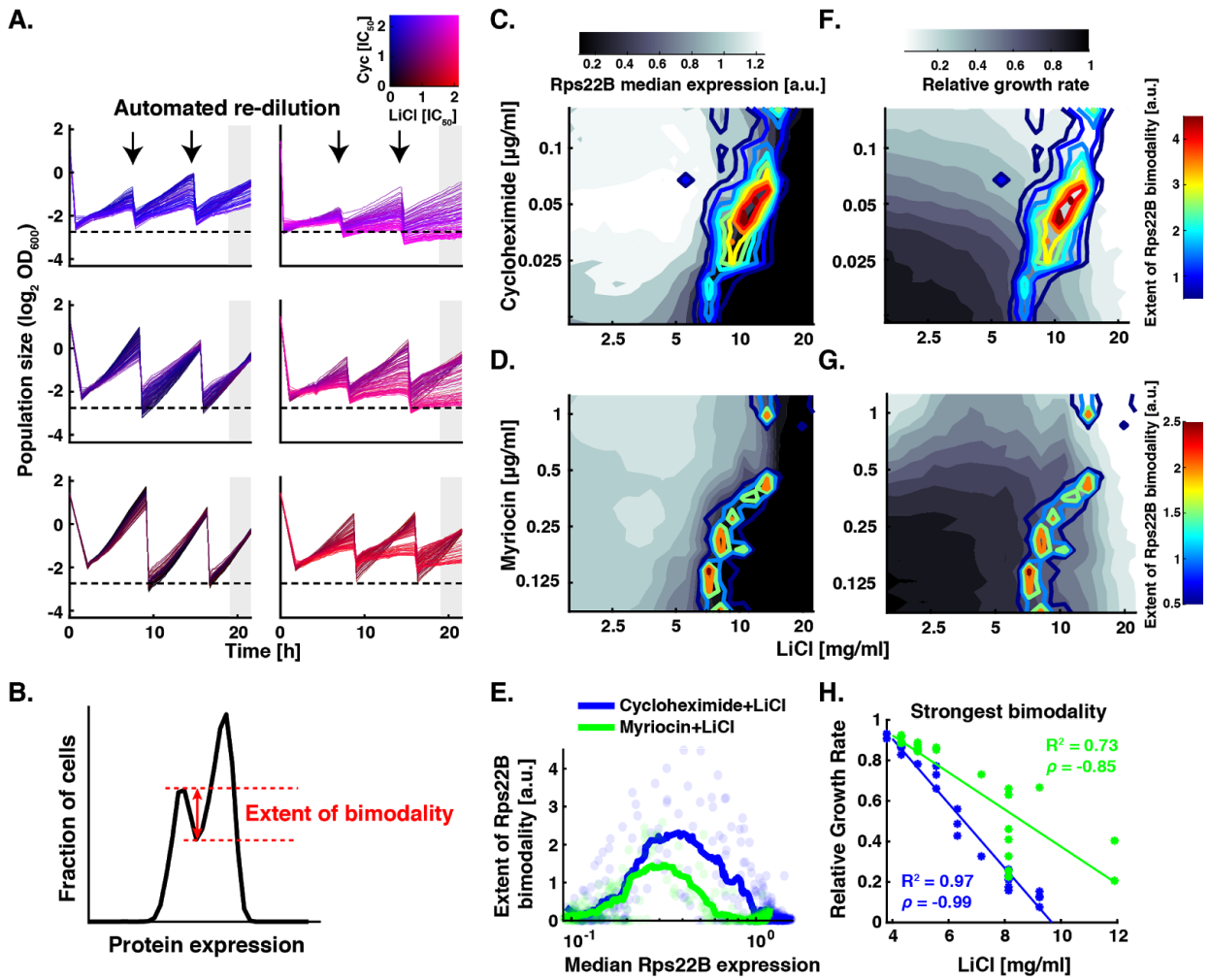

Figure S4: Rps22B protein expression is consistent with a bistable regulatory loop.

A. Growth curves from the automated re-inoculation setup of cultures growing in a detailed 2-drug gradient of LiCl and cycloheximide, spread over 576 wells of six microtitre plates. Each panel shows growth curves for cultures on one 96-well plate. Drops in OD_{600} are due to automated re-dilution of growing cultures to an arbitrary target OD (dashed line). Shaded area denotes measurements that were used to determine the exponential growth rates shown in F. and G. **B.** Schematic showing the definition of the metric used to analyse the Rps22B bimodal expression pattern. The extent of bimodality is defined here as the y-axis distance between the trough and the lower of the two peaks on the histogram of single-cell protein expression, with bin size kept consistent throughout the analysis. For technical definition see *Methods*. **C. and D.** The extent of Rps22B bimodality (coloured lines), is overlaid on Rps22B median expression (grayscale) in a 2-drug gradient of LiCl and cycloheximide (C) or myriocin (D). **E.** Rps22B protein bimodality as a function of median Rps22B protein expression for all wells in the 2-drug gradient (dots) is shown alongside with running average with a window of 30 data points (lines). Rps22B bimodality peaks at a certain level of median Rps22B expression, rather than at a certain growth rate or LiCl concentration. **F. and G.** The extent of Rps22B bimodality (coloured lines) is overlaid on growth rate (grayscale) in a 2D gradient of LiCl and cycloheximide (F) or myriocin (G). **H.** For each concentration of cycloheximide (blue) or myriocin (green), the LiCl concentration that elicited maximum Rps22B protein bimodality is plotted, with corresponding growth rate of the culture. The strength of LiCl stress needed to bring the level of Rps22B to the putative unstable fixed point is inversely dependent on the growth rate, suggesting that the Rps22B switch is quantitatively attuned to specific growth conditions. ρ – Pearson correlation coefficient. See also **Fig. S5** for Rps22B single-cell gene expression data for individual wells.

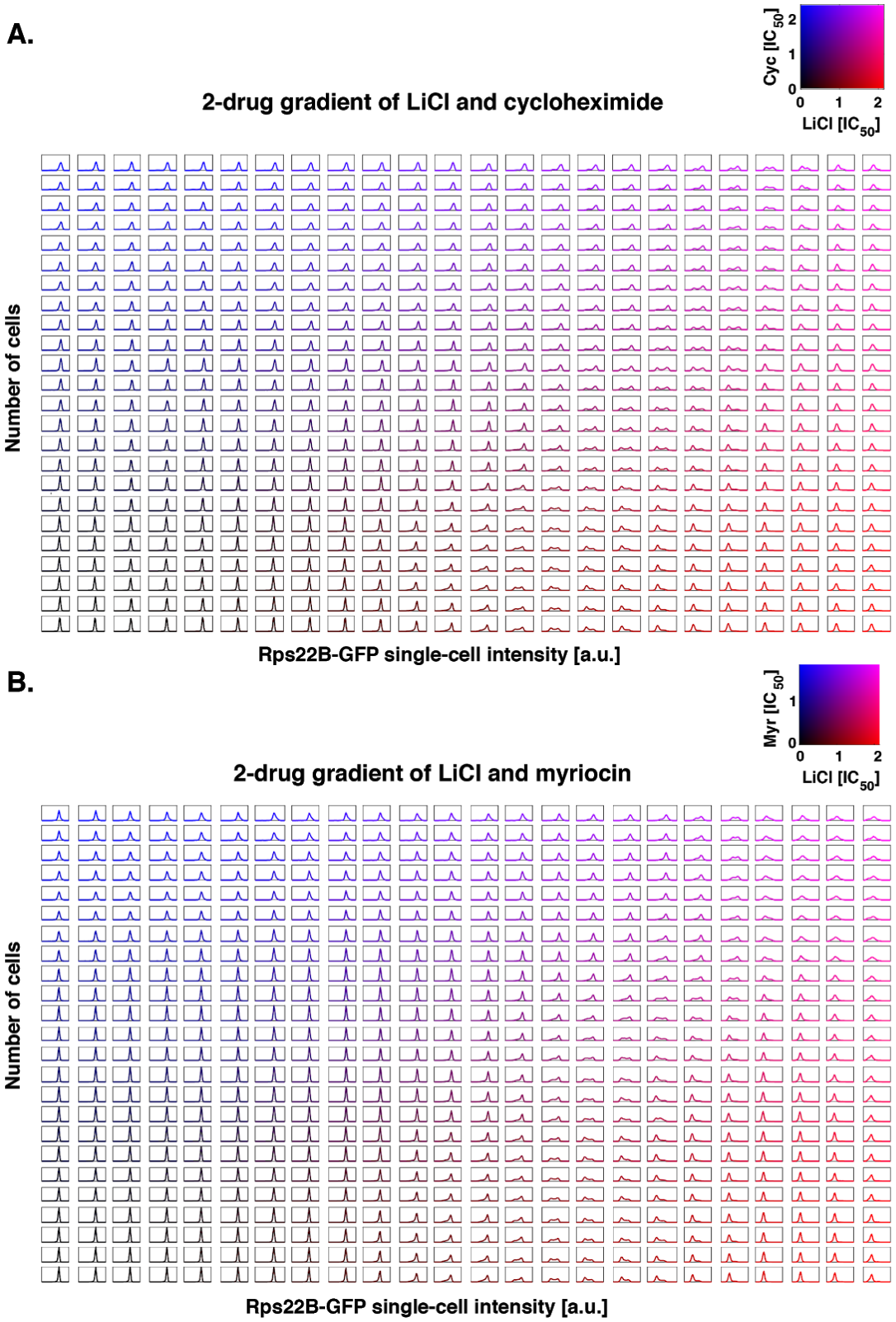

Figure S5: Rps22B single-cell protein expression in a detailed 2-drug gradient. Refers to Figure 2.

A. Histograms for 576 cultures with graded levels of LiCl and cycloheximide, incubated by automated reinoculation protocol.

B. Same as in A, except for LiCl and myriocin.

Supplementary tables

Table S1: Flow cytometry summary data for strains from the yeast protein-GFP library profiled in four conditions. For each profiled strain and condition, the summary statistics for FITC-H channel normalized cell-wise to FSC-H channel is listed, including arithmetic mean, standard deviation, and relative counts in 100 histogram bins spaced logarithmically from 1e-3 to 1e5. The strains that were profiled in the more detailed 8-point measurement (**Table S2**), are not listed.

Table S2: Flow cytometry summary data for strains from the yeast protein-GFP library profiled in eight conditions. For each profiled strain and condition, the summary statistics for FITC-H channel normalized cell-wise to FSC-H channel is listed, including arithmetic mean, standard deviation, and relative counts in 100 histogram bins spaced logarithmically from 1e-3 to 1e5. The measurement of parent BY4741 (non-GFP) strain is listed as well for background fluorescence reference.

References

1. Metzl-Raz, E. *et al.* Principles of cellular resource allocation revealed by condition-dependent proteome profiling. *eLife* **6**, e28034 (2017).
2. Scott, M., Klumpp, S., Mateescu, E. M. & Hwa, T. Emergence of robust growth laws from optimal regulation of ribosome synthesis. *Mol. Syst. Biol.* **10**, (2014).
3. Soria, P. S., McGary, K. L. & Rokas, A. Functional Divergence for Every Paralog. *Mol. Biol. Evol.* **31**, 984–992 (2014).
4. Evangelisti, A. M. & Conant, G. C. Nonrandom Survival of Gene Conversions among Yeast Ribosomal Proteins Duplicated through Genome Doubling. *Genome Biol. Evol.* **2**, 826–834 (2010).
5. Parenteau, J. *et al.* Preservation of Gene Duplication Increases the Regulatory Spectrum of Ribosomal Protein Genes and Enhances Growth under Stress. *Cell Rep.* **13**, 2516–2526 (2015).
6. Morgan, J. T., Fink, G. R. & Bartel, D. P. Excised linear introns regulate growth in yeast. *Nature* **565**, 606 (2019).
7. Parenteau, J. *et al.* Introns are mediators of cell response to starvation. *Nature* **565**, 612 (2019).
8. Parenteau, J. *et al.* Introns within Ribosomal Protein Genes Regulate the Production and Function of Yeast Ribosomes. *Cell* **147**, 320–331 (2011).
9. Lukačišin, M. & Bollenbach, T. Emergent Gene Expression Responses to Drug Combinations Predict Higher-Order Drug Interactions. *Cell Syst.* **9**, 423-433.e3 (2019).
10. Huh, W.-K. *et al.* Global analysis of protein localization in budding yeast. *Nature* **425**, 686–691 (2003).
11. Levy, S. F., Ziv, N. & Siegal, M. L. Bet Hedging in Yeast by Heterogeneous, Age-Correlated Expression of a Stress Protectant. *PLOS Biol.* **10**, e1001325 (2012).
12. Breker, M., Gymrek, M. & Schuldiner, M. A novel single-cell screening platform reveals proteome plasticity during yeast stress responses. *J Cell Biol* **200**, 839–850 (2013).
13. Chapal, M., Mintzer, S., Brodsky, S., Carmi, M. & Barkai, N. Resolving noise–control conflict by gene duplication. *PLOS Biol.* **17**, e3000289 (2019).
14. Hughes, T. R. *et al.* Widespread aneuploidy revealed by DNA microarray expression profiling. *Nat. Genet.* **25**, 333–337 (2000).
15. Thomson, E., Ferreira-Cerca, S. & Hurt, E. Eukaryotic ribosome biogenesis at a glance. *J. Cell Sci.* **126**, 4815–4821 (2013).
16. Pelletier, J., Thomas, G. & Volarević, S. Ribosome biogenesis in cancer: new players and therapeutic avenues. *Nat. Rev. Cancer* **18**, 51–63 (2018).
17. Warner, J. R. The economics of ribosome biosynthesis in yeast. *Trends Biochem. Sci.* **24**, 437–440 (1999).
18. Kellis, M., Birren, B. W. & Lander, E. S. Proof and evolutionary analysis of ancient genome duplication in the yeast *Saccharomyces cerevisiae*. *Nature* **428**, 617–624 (2004).
19. Marcet-Houben, M. & Gabaldón, T. Beyond the Whole-Genome Duplication: Phylogenetic Evidence for an Ancient Interspecies Hybridization in the Baker's Yeast Lineage. *PLOS Biol.* **13**, e1002220 (2015).
20. Mullis, A. *et al.* Parallel Concerted Evolution of Ribosomal Protein Genes in Fungi and Its Adaptive Significance. *Mol. Biol. Evol.* **37**, 455–468 (2020).
21. Gu, Z. *et al.* Role of duplicate genes in genetic robustness against null mutations. *Nature* **421**, 63–66 (2003).
22. Ghulam, M. M., Catala, M. & Abou Elela, S. Differential expression of duplicated ribosomal protein genes modifies ribosome composition in response to stress. *Nucleic Acids Res.* **48**, 1954–1968

(2020).
23. Petibon, C., Parenteau, J., Catala, M. & Elela, S. A. Introns regulate the production of ribosomal proteins by modulating splicing of duplicated ribosomal protein genes. *Nucleic Acids Res.* **44**, 3878–3891 (2016).
24. Xue, S. & Barna, M. Specialized ribosomes: a new frontier in gene regulation and organismal biology. *Nat. Rev. Mol. Cell Biol.* **13**, 355–369 (2012).
25. Ascencio, D., Ochoa, S., Delaye, L. & DeLuna, A. Increased rates of protein evolution and asymmetric deceleration after the whole-genome duplication in yeasts. *BMC Evol. Biol.* **17**, 40 (2017).
26. DeLuna, A., Springer, M., Kirschner, M. W. & Kishony, R. Need-Based Up-Regulation of Protein Levels in Response to Deletion of Their Duplicate Genes. *PLOS Biol.* **8**, e1000347 (2010).
27. Wapinski, I. *et al.* Gene duplication and the evolution of ribosomal protein gene regulation in yeast. *Proc. Natl. Acad. Sci.* **107**, 5505–5510 (2010).
28. Komili, S., Farny, N. G., Roth, F. P. & Silver, P. A. Functional Specificity among Ribosomal Proteins Regulates Gene Expression. *Cell* **131**, 557–571 (2007).
29. Hooks, K. B., Delneri, D. & Griffiths-Jones, S. Intron Evolution in Saccharomycetaceae. *Genome Biol. Evol.* **6**, 2543–2556 (2014).
30. Vilardell, J. & Warner, J. R. Regulation of splicing at an intermediate step in the formation of the spliceosome. *Genes Dev.* **8**, 211–220 (1994).
31. Vilardell, J., Chartrand, P., Singer, R. H. & Warner, J. R. The odyssey of a regulated transcript. *RNA* **6**, 1773–1780 (2000).
32. Pleiss, J. A., Whitworth, G. B., Bergkessel, M. & Guthrie, C. Rapid, Transcript-Specific Changes in Splicing in Response to Environmental Stress. *Mol. Cell* **27**, 928–937 (2007).
33. Brauer, M. J. *et al.* Coordination of Growth Rate, Cell Cycle, Stress Response, and Metabolic Activity in Yeast. *Mol. Biol. Cell* **19**, 352–367 (2008).
34. Phiel, C. J. & Klein, P. S. Molecular Targets of Lithium Action. *Annu. Rev. Pharmacol. Toxicol.* **41**, 789–813 (2001).
35. Schneider-Poetsch, T. *et al.* Inhibition of Eukaryotic Translation Elongation by Cycloheximide and Lactimidomycin. *Nat. Chem. Biol.* **6**, 209–217 (2010).
36. Sayani, S., Janis, M., Lee, C. Y., Toesca, I. & Chanfreau, G. F. Widespread Impact of Nonsense-Mediated mRNA Decay on the Yeast Intronome. *Mol. Cell* **31**, 360–370 (2008).
37. Roy, B. *et al.* Autoregulation of yeast ribosomal proteins discovered by efficient search for feedback regulation. *Commun. Biol.* **3**, 1–9 (2020).
38. Yaakov, G., Lerner, D., Bentele, K., Steinberger, J. & Barkai, N. Coupling phenotypic persistence to DNA damage increases genetic diversity in severe stress. *Nat. Ecol. Evol.* **1**, s41559-016-0016–016 (2017).
39. Avbelj, M., Zupan, J., Kranjc, L. & Raspor, P. Quorum-Sensing Kinetics in Saccharomyces cerevisiae: A Symphony of ARO Genes and Aromatic Alcohols. *J. Agric. Food Chem.* **63**, 8544–8550 (2015).
40. Chen, H. & Fink, G. R. Feedback control of morphogenesis in fungi by aromatic alcohols. *Genes Dev.* **20**, 1150–1161 (2006).
41. Sprague, G. F. & Winans, S. C. Eukaryotes learn how to count: quorum sensing by yeast. *Genes Dev.* **20**, 1045–1049 (2006).
42. Birtwistle, M. R. *et al.* Emergence of bimodal cell population responses from the interplay between analog single-cell signaling and protein expression noise. *BMC Syst. Biol.* **6**, 109 (2012).
43. To, T.-L. & Maheshri, N. Noise can induce bimodality in positive transcriptional feedback loops without bistability. *Science* **327**, 1142–1145 (2010).

44. Strogatz, S. H. *Nonlinear dynamics and chaos: with applications to physics, biology, chemistry, and engineering*. (CRC Press, 2018).
45. Miyake, Y., Kozutsumi, Y., Nakamura, S., Fujita, T. & Kawasaki, T. Serine palmitoyltransferase is the primary target of a sphingosine-like immunosuppressant, ISP-1/myriocin. *Biochem. Biophys. Res. Commun.* **211**, 396–403 (1995).
46. Boulon, S., Westman, B. J., Hutten, S., Boisvert, F.-M. & Lamond, A. I. The Nucleolus under Stress. *Mol. Cell* **40**, 216–227 (2010).
47. Bagamery, L. E., Justman, Q. A., Garner, E. C. & Murray, A. W. Bet hedging buffers budding yeast against environmental instability. *bioRxiv* 2020.04.08.032904 (2020) doi:10.1101/2020.04.08.032904.
48. Mitchell, A. *et al.* Adaptive prediction of environmental changes by microorganisms. *Nature* **460**, 220–224 (2009).
49. Gomar-Alba, M., Morcillo-Parra, M. Á. & Olmo, M. del. Response of yeast cells to high glucose involves molecular and physiological differences when compared to other osmostress conditions. *FEMS Yeast Res.* **15**, (2015).
50. Santos, J., Leitão-Correia, F., Sousa, M. J. & Leão, C. Nitrogen and carbon source balance determines longevity, independently of fermentative or respiratory metabolism in the yeast Saccharomyces cerevisiae. *Oncotarget* **7**, 23033–23042 (2016).
51. Yu, R. *et al.* Nitrogen limitation reveals large reserves in metabolic and translational capacities of yeast. *Nat. Commun.* **11**, 1881 (2020).
52. Liu, H.-F., Wu, B.-H., Fan, P.-G., Li, S.-H. & Li, L.-S. Sugar and acid concentrations in 98 grape cultivars analyzed by principal component analysis. *J. Sci. Food Agric.* **86**, 1526–1536 (2006).
53. Bergkessel, M., Whitworth, G. B. & Guthrie, C. Diverse environmental stresses elicit distinct responses at the level of pre-mRNA processing in yeast. *RNA* **17**, 1461–1478 (2011).
54. Considine, J. A. & Kriedemann, P. E. Fruit splitting in grapes: Determination of the critical turgor pressure. *Aust. J. Agric. Res.* **23**, 17–23 (1972).
55. Ramteke, S. D., Urkude, V., Parhe, S. D. & Bhagwat, S. R. Berry cracking; its causes and remedies in grapes - A Review. *Trends Biosci.* **10**, 549–556 (2017).
56. Hoshida, H., Kondo, M., Kobayashi, T., Yarimizu, T. & Akada, R. 5´-UTR introns enhance protein expression in the yeast Saccharomyces cerevisiae. *Appl. Microbiol. Biotechnol.* **101**, 241–251 (2017).
57. Kim, D. *et al.* TopHat2: accurate alignment of transcriptomes in the presence of insertions, deletions and gene fusions. *Genome Biol.* **14**, R36 (2013).
58. Liao, Y., Smyth, G. K. & Shi, W. featureCounts: an efficient general purpose program for assigning sequence reads to genomic features. *Bioinforma. Oxf. Engl.* **30**, 923–930 (2014).
59. Eden, E., Navon, R., Steinfeld, I., Lipson, D. & Yakhini, Z. GOrilla: a tool for discovery and visualization of enriched GO terms in ranked gene lists. *BMC Bioinformatics* **10**, 48 (2009).
60. Howson, R. *et al.* Construction, verification and experimental use of two epitope-tagged collections of budding yeast strains. *Comp. Funct. Genomics* **6**, 2–16 (2005).
61. Kamentsky, L. *et al.* Improved structure, function and compatibility for CellProfiler: modular high-throughput image analysis software. *Bioinformatics* **27**, 1179–1180 (2011).